Valence-band warping in tight-binding models

Timothy B. Boykin and Lisa J. Gamble
Department of Electrical and Computer Engineering and LICOS, The University of Alabama in Huntsville, Huntsville, Alabama 35899

Gerhard Klimeck and R. Chris Bowen
Jet Propulsion Laboratory, California Institute of Technology, 4800 Oak Grove Drive, MS 168-522, Pasadena, California 91109-8099
(Received 24 August 1998)

The spin-orbit nearest-neighbor sp^3s^* model is widely believed able to reproduce accurately the valence bands of most III-V and group-IV semiconductors, essential for modeling the in-plane dispersion of valence- and inter-band quantum heterostructures. To check this belief, we study valence-band warping in the spin-orbit sp^3s^* model including interactions up to second-nearest-neighbor, providing exact, analytic formulas for the [110] and [111] light- and heavy-hole masses. Surprisingly, we find that the second-nearest-neighbor model offers significantly more flexibility in fitting these masses independently of those along [001] than does the nearest-neighbor model. [S0163-1829(99)10007-9]

Empirical tight-binding techniques are increasingly employed in calculating the transport and optical properties of quantum semiconductor structures such as resonant-tunneling diodes (RTDs), quantum wells (QW's), and superlattices. Being relatively more complete than envelope-function or $\mathbf{k}\cdot\mathbf{p}$ models, they naturally incorporate the entire bandstructure of the constituent bulk materials in a transparent manner; the short-range nature of their interactions also facilitates modeling the heterointerfaces present in such structures. Judiciously employed, the tight-binding method can deliver results of high accuracy; all too often, however, this potential goes unrealized, through a poor choice of either model or parameters. Indeed, while it ought to be self-evident, or at least easily deduced from the derivatives of the Hamiltonian matrix,[1] the incompleteness of any practical tight-binding model is effectively ignored by many scientists. This notwithstanding, the tight-binding technique remains a powerful and subtle approximation method, requiring care in its application, especially regarding the choice and parametrization of models.

In order to help workers choose and optimize tight-binding models we have recently studied the properties of the spin-orbit sp^3s^* model[2] in both its nearest-[3] and second-nearest[4]-neighbor manifestations, presenting exact formulas for the effective masses along [001]. Formulas for the effective masses along [001] in the no-spin orbit, second-near-neighbor sp^3 model have been given by Loehr and Talwar.[5] These studies, through their analytic expressions showing the exact parameter dependence of the curvatures, have greatly improved the understanding of the relationship between the electron- and light-hole masses. Results of these efforts include parametrizations more accurately reproducing the complex bands of QW and RTD barrier materials, essential for good conduction-band device calculations, as well as a better appreciation for the propriety of a given model (nearest- vs second-nearest neighbor) for a given material.

As useful as these analytic formulas are, however, they need to be supplemented for work involving valence- or interband heterostructures due to the significant warping of the heavy-hole bands along the [110] and [111] directions. This warping is important for valence-band QWs grown on [001]-oriented substrates, since it affects the in-plane dispersion of the bound states, a subject of theoretical interest;[6,7] more intriguingly, recent experiments employing resonant magnetotunneling spectroscopy[8–11] have directly probed the QW in-plane dispersion. Correct calculation of valence-band states, therefore, demands good reproduction of the hole masses in all three directions, which requires that the exact relationship between the masses be understood. It is particularly important to determine whether or not fixing the heavy- and light-hole masses in one direction determines them in the others. Also, since the second-near-neighbor model is more computationally demanding than the nearest-neighbor version it is of interest to know whether or not it can more accurately reproduce the hole masses along each direction. Finally, in fitting the parameters of a tight-binding model, the more is known about the masses, the easier the process. Addressing all of these issues, therefore, requires not only exact analytic expressions for the [110] and [111] masses but also a thorough understanding of their connection to the [001] masses.

We consider the sp^3s^* Hamiltonian[2] with interactions up to the second-nearest neighbor. We follow Chadi's[12] treatment of the spin-orbit coupling, which retains only same-site spin-orbit parameters, since in most materials the shift of the heavy-hole maxima away from the zone center is not significant. (Reproducing this shift requires at least nearest-neighbor spin-orbit coupling,[13] and furthermore, renders analytic effective mass formulas impractical at the very minimum since the valence-band maxima no longer occur at $\mathbf{k}=\mathbf{0}$.) We furthermore assume that both the nearest- and second-nearest neighbor s-s^* and s^*-s^* parameters are set to zero. Our nonzero parameters, in the Slater-Koster[14] notation, along with abbreviations for those appearing in the effective-mass formulas, are given in Table I.

Using the method of Ref. 1 we determine the inverse effective masses. Since the matrix $\nabla_{\mathbf{k}}H(\mathbf{k})$ does not lift the degeneracy, we must diagonalize the curvature matrix in the fourfold-degenerate subspace $\{|\mathrm{LH};1\rangle,|\mathrm{HH};1\rangle,|\mathrm{LH};2\rangle, |\mathrm{HH};2\rangle\}$; for consistency of notation we continue to employ

TABLE I. Nonzero tight-binding parameters (notation of Ref. 14) along with our abbreviations; units are eV.

Abbreviation	Parameter	GaAs	GaSb	InSb
E_{sa}	$E^{(000)}_{sa,sa}$	−8.487 06	−4.974 14	−8.781 10
E_{pa}	$E^{(000)}_{pa,pa}$	0.387 69	0.591 30	0.508 90
E_{s^*a}	$E^{(000)}_{s^*a,s^*a}$	8.487 69	8.150 00	7.409 90
E_{sc}	$E^{(000)}_{sc,sc}$	−2.861 11	−2.604 92	−2.497 90
E_{pc}	$E^{(000)}_{pc,pc}$	3.567 69	3.240 86	3.306 10
E_{s^*c}	$E^{(000)}_{s^*c,s^*c}$	6.617 69	6.666 75	6.740 10
$V_{s,s}$	$4E^{(1/2\ 1/2\ 1/2)}_{sa,sc}$	−6.460 53	−4.820 00	−5.395 30
$V_{sa,pc}$	$4E^{(1/2\ 1/2\ 1/2)}_{sa,pc}$	4.680 00	3.808 36	2.335 40
$V_{s^*a,pc}$	$4E^{(1/2\ 1/2\ 1/2)}_{s^*a,pc}$	4.650 00	4.757 93	2.498 40
$V_{pa,sc}$	$4E^{(1/2\ 1/2\ 1/2)}_{pa,sc}$	8.000 00	6.978 62	6.338 90
V_{pa,s^*c}	$4E^{(1/2\ 1/2\ 1/2)}_{pa,s^*c}$	6.000 00	5.366 84	3.909 70
$V_{x,x}$	$4E^{(1/2\ 1/2\ 1/2)}_{x,x}$	2.260 95	1.893 76	1.839 80
$V_{x,y}$	$4E^{(1/2\ 1/2\ 1/2)}_{x,y}$	5.170 00	4.610 63	4.469 30
$V_{sa,sa}$	$4E^{(110)}_{sa,sa}$	−0.010 00	−0.018 60	−0.009 00
$V_{sa,xa}$	$4E^{(110)}_{sa,xa}$	0.050 00	0.043 10	0.045 00
	$4E^{(011)}_{sa,xa}$	0.058 00	0.050 00	0.052 20
$V_{s^*a,xa}$	$4E^{(110)}_{s^*a,xa}$	0.020 00	0.017 24	0.018 00
	$4E^{(011)}_{s^*a,xa}$	0.040 00	0.034 48	0.036 00
$V_{xa,xa}$	$4E^{(110)}_{xa,xa}$	0.320 00	0.275 90	0.288 00
$U_{xa,xa}$	$4E^{(011)}_{xa,xa}$	−0.050 00	−0.043 10	−0.045 00
$V_{xa,ya}$	$4E^{(110)}_{xa,ya}$	0.640 00	0.569 00	0.210 00
	$4E^{(011)}_{xa,ya}$	−1.000 00	−0.862 10	−0.900 00
$V_{sc,sc}$	$4E^{(110)}_{sc,sc}$	−0.020 00	−0.032 24	−0.018 00
$V_{sc,xc}$	$4E^{(110)}_{sc,xc}$	0.072 00	0.062 07	0.064 80
	$4E^{(011)}_{sc,xc}$	0.020 00	0.017 24	0.018 00
$V_{s^*c,xc}$	$4E^{(110)}_{s^*c,xc}$	0.010 00	0.008 62	0.009 00
	$4E^{(011)}_{s^*c,xc}$	0.093 50	0.080 61	0.084 15
$V_{xc,xc}$	$4E^{(110)}_{xc,xc}$	0.280 00	0.215 50	0.252 00
$U_{xc,xc}$	$4E^{(011)}_{xc,xc}$	−0.100 00	−0.086 21	−0.090 00
$V_{xc,yc}$	$4E^{(110)}_{xc,yc}$	0.200 00	0.445 00	0.110 00
	$4E^{(011)}_{xc,yc}$	−1.300 00	−1.120 70	−1.170 00
	λ_a	0.140 00	0.324 33	0.324 33
	λ_c	0.058 00	0.058 00	0.131 00

the states given in Ref. 13. The algebra is straightforward but rather tedious; each mass is doubly degenerate. Although the resulting expressions for the [110] masses in terms of the tight-binding parameters are quite complicated and do not convey much insight, when recast in terms of the other masses they reveal a great deal about the properties inherent in the nearest- and second-nearest neighbor sp^3s^* models; the [111] masses are considerably simpler. Carrying out this calculation, we find for the [111] masses[15]

$$\frac{m_0}{m^{(\mathrm{hh})}_{[111]}}=\left(\frac{2m_0}{\hbar^2}\right)\left(\frac{a}{4}\right)^2\left(\frac{1}{3}\right)[4(\rho_a^{l,+})^2(V_{xc,yc}-2V_{xc,xc}-U_{xc,xc})+4(\rho_c^{l,+})^2(V_{xa,ya}-2V_{xa,xa}-U_{xa,xa})-\rho_a^{l,+}\rho_c^{l,+}(V_{x,y}+3V_{x,x})(V_{x,y}-V_{x,x})/V_{x,x}], \quad (1)$$

$$\frac{m_0}{m^{(\mathrm{lh})}_{[111]}}=\frac{m_0}{m^{(\mathrm{lh})}_{[001]}}+\frac{m_0}{m^{(\mathrm{hh})}_{[001]}}-\frac{m_0}{m^{(\mathrm{hh})}_{[111]}}, \quad (2)$$

where a is the conventional unit-cell cube edge, m_0 the free-electron mass, and $m^{(\mathrm{lh})}_{[001]}$ and $m^{(\mathrm{hh})}_{[001]}$ the effective masses for light and heavy holes along [001], given in Eqs. (5) and (6) of Ref. 4, respectively. The coefficients ρ are likewise the same as in Ref. 4:

$$\rho_a^{l,+}=\frac{E_\Delta^{(\mathrm{lh})}+\Delta^{(\mathrm{lh})}}{\sqrt{2}\sqrt{\Delta^{(\mathrm{lh})^2}+E_\Delta^{(\mathrm{lh})}\Delta^{(\mathrm{lh})}}},$$

$$\rho_c^{l,+}=\frac{V_{x,x}}{\sqrt{2}\sqrt{\Delta^{(\mathrm{lh})^2}+E_\Delta^{(\mathrm{lh})}\Delta^{(\mathrm{lh})}}}, \quad (3)$$

TABLE II. Energy gaps (eV) and effective masses (m_0) reproduced by the parameters of Table I and Ref. 4 (GaAs only). $E_{X\Gamma}$ and $E_{L\Gamma}$ are the gaps between the conduction-band X- and L-valley minima and the Γ-valley minimum, respectively. The superscripts c, lh, hh, and soh respectively, refer to the conduction, and light-, heavy-, and split-off-hole masses.

Quantity	GaAs	GaAs-Ref. 4	GaSb	InSb
$E_g(\Gamma)$	1.424	1.424	0.754	0.169
$E_{X\Gamma}$	0.482	0.482	0.443	1.493
$E_{L\Gamma}$	0.597	0.313	0.437	0.931
Δ_0	0.366	0.366	0.800	0.857
$m^{(c)}_\Gamma$	0.068	0.068	0.048	0.013
$m^{(c)}_{X,l}$	1.317	1.317	1.303	1.043
$m^{(c)}_{X,t}$	0.314	0.314	0.334	0.210
$m^{(c)}_{L,l}$	1.724	1.392	1.509	1.439
$m^{(c)}_{L,t}$	0.194	0.129	0.159	0.111
$\lvert m^{(\mathrm{lh})}_{[001]}\rvert$	0.071	0.071	0.050	0.013
$\lvert m^{(\mathrm{lh})}_{[110]}\rvert$	0.066	0.065	0.047	0.013
$\lvert m^{(\mathrm{lh})}_{[111]}\rvert$	0.065	0.063	0.046	0.013
$\lvert m^{(\mathrm{hh})}_{[001]}\rvert$	0.412	0.412	0.356	0.321
$\lvert m^{(\mathrm{hh})}_{[110]}\rvert$	0.695	0.882	0.622	0.497
$\lvert m^{(\mathrm{hh})}_{[111]}\rvert$	0.877	1.331	0.808	0.606
$\lvert m^{(\mathrm{soh})}\rvert$	0.144	0.144	0.151	0.120

$$\Delta^{(\mathrm{lh})}=\sqrt{{E_{\Delta}^{(\mathrm{lh})}}^2+{V_{x,x}}^2},\quad E_{\Delta}^{(\mathrm{lh})}=\tfrac{1}{2}(E_a-E_c),$$

$$E_{\mu}=E_{p\mu}+2V_{x\mu,x\mu}+U_{x\mu,x\mu}+\lambda_{\mu},\mu\in\{a,c\}. \tag{4}$$

In contrast, we find that the [110] masses can be expressed without explicit reference to the tight-binding parameters:

$$\frac{m_0}{m_{[110]}^{(\mathrm{hh})}}=\frac{1}{2}\left(\frac{m_0}{m_{[001]}^{(\mathrm{lh})}}+\frac{m_0}{m_{[001]}^{(\mathrm{hh})}}\right)+\left\{\frac{1}{16}\left(\frac{m_0}{m_{[001]}^{(\mathrm{lh})}}-\frac{m_0}{m_{[001]}^{(\mathrm{hh})}}\right)^2+\frac{3}{4}\left[\frac{1}{2}\left(\frac{m_0}{m_{[001]}^{(\mathrm{lh})}}+\frac{m_0}{m_{[001]}^{(\mathrm{hh})}}\right)-\frac{m_0}{m_{[111]}^{(\mathrm{hh})}}\right]^2\right\}^{1/2}, \tag{5}$$

$$\frac{m_0}{m_{[110]}^{(\mathrm{lh})}}=\frac{1}{2}\left(\frac{m_0}{m_{[001]}^{(\mathrm{lh})}}+\frac{m_0}{m_{[001]}^{(\mathrm{hh})}}\right)-\left\{\frac{1}{16}\left(\frac{m_0}{m_{[001]}^{(\mathrm{lh})}}-\frac{m_0}{m_{[001]}^{(\mathrm{hh})}}\right)^2+\frac{3}{4}\left[\frac{1}{2}\left(\frac{m_0}{m_{[001]}^{(\mathrm{lh})}}+\frac{m_0}{m_{[001]}^{(\mathrm{hh})}}\right)-\frac{m_0}{m_{[111]}^{(\mathrm{hh})}}\right]^2\right\}^{1/2}$$

$$=\frac{m_0}{m_{[001]}^{(\mathrm{lh})}}+\frac{m_0}{m_{[001]}^{(\mathrm{hh})}}-\frac{m_0}{m_{[110]}^{(\mathrm{hh})}}. \tag{6}$$

Note that the hole masses in Eqs. (1), (2), (5), and (6) are negative.

The implications of Eqs. (1), (2), (5), and (6) for both the choice and parametrization of a tight-binding model are profound indeed. In the first place, we see from Eq. (1) that the *only* parameters *not* appearing in the expressions for $m_{[001]}^{(\mathrm{lh})}$ and $m_{[001]}^{(\mathrm{hh})}$ are the second-nearest-neighbor interactions $V_{xa,ya}$ and $V_{xc,yc}$. Indeed, in the nearest-neighbor model both $m_{[001]}^{(\mathrm{hh})}$ and $m_{[111]}^{(\mathrm{hh})}$ are determined by only six parameters (E_{pa}, E_{pc}, $V_{x,x}$, $V_{x,y}$, λ_a, and λ_c) of which two, λ_a and λ_c are, for all practical purposes fixed, while each of the remaining four affects at least one of these features: the gaps at Γ and X, the light-hole masses, the conduction-band mass at Γ, and the X-valley longitudinal mass. Thus, although it is certainly true that a nearest-neighbor model can reproduce both $m_{[001]}^{(\mathrm{hh})}$ and $m_{[111]}^{(\mathrm{hh})}$, it is also obvious that doing so may entail significant compromises in one or more of these other band-structure features, so that for valence- and interband heterostructures the second-nearest-neighbor model may be the better choice. Furthermore, since Eqs. (2), (5), and (6) are expressed *solely* in terms of $m_{[001]}^{(\mathrm{lh})}$, $m_{[001]}^{(\mathrm{hh})}$, and $m_{[111]}^{(\mathrm{hh})}$ we see that, in spite of the entry of two new parameters into Eq. (1), these three masses specify *completely* the remaining three (not just two). Indeed, the fact that only the second-nearest-neighbor model offers additional freedom (and only via the parameters $V_{xa,ya}$ and $V_{xc,yc}$) in fitting the [110] and [111] masses is a bit surprising in view of the widely held perception that even the nearest-neighbor sp^3 model can accurately fit the *valence* bands.

The above formulas give us further insight into properties of the model; from Eq. (1) we can see that the [111] heavy-hole mass will usually be greater in magnitude than the [001] heavy-hole mass. The first two terms of Eq. (1), the second-order corrections due to second-near-neighbor interactions, are (with the global factor $\frac{1}{3}$) more positive/less negative generally than those of the [001] expression due to the newly appearing parameters $V_{xa,ya}$ and $V_{xc,yc}$, tending to make the [111] holes heavier than the [001] holes. The last term of Eq. (1) likewise tends toward heavier holes; rewriting it,[15]

$$-\rho_a^{l,+}\rho_c^{l,+}\frac{(V_{x,y}+3V_{x,x})(V_{x,y}-V_{x,x})}{V_{x,x}}=3\rho_a^{l,+}\rho_c^{l,+}V_{x,x}+\frac{{V_{x,y}}^2}{E_-^{(\mathrm{lh})}-E_+^{(\mathrm{lh})}}+2\frac{V_{x,y}V_{x,x}}{E_-^{(\mathrm{lh})}-E_+^{(\mathrm{lh})}}. \tag{7}$$

We see that (again accounting for the global factor $\frac{1}{3}$) the first two terms of Eq. (7) are the same as their counterparts in the [001] expression. The last term of Eq. (7) is, like the heavy-hole split-off electron term of the [001] expression, negative, but in the limit of small spin-orbit coupling it is smaller in magnitude by approximately $V_{x,x}/V_{x,y}$, therefore increasing the curvature rather less than in the [001] case. (The remaining term of the [001] case is the typically quite small heavy-hole split-off hole coupling.) Altogether, then, these trends tend to make the [111] heavy holes heavier than the [001] heavy holes, regardless of the parameters.

Because the heavy-hole mass is in most materials considerably larger than the light-hole mass, Taylor expansions of Eqs. (5) and (6) can give further insight into the interrelationships among the masses intrinsic to the models. To the first order in $m_{[001]}^{(\mathrm{lh})}/m_{[001]}^{(\mathrm{hh})}$ and $m_{[001]}^{(\mathrm{lh})}/m_{[111]}^{(\mathrm{hh})}$,

$$\frac{m_0}{m_{[110]}^{(\mathrm{lh})}}\approx\frac{m_0}{m_{[001]}^{(\mathrm{lh})}}+\frac{3}{4}\left(\frac{m_0}{m_{[001]}^{(\mathrm{hh})}}-\frac{m_0}{m_{[111]}^{(\mathrm{hh})}}\right), \tag{8}$$

$$\frac{m_0}{m_{[110]}^{(\mathrm{hh})}}\approx\frac{1}{4}\frac{m_0}{m_{[001]}^{(\mathrm{hh})}}+\frac{3}{4}\frac{m_0}{m_{[111]}^{(\mathrm{hh})}}. \tag{9}$$

From these we see that $m_{[110]}^{(\mathrm{lh})}$ is usually close to $m_{[001]}^{(\mathrm{lh})}$ and that $m_{[110]}^{(\mathrm{hh})}$ lies closer to $m_{[111]}^{(\mathrm{hh})}$ than $m_{[001]}^{(\mathrm{hh})}$; these trends are generally reflective of experimental results to the extent that the model employed accurately fits $m_{[111]}^{(\mathrm{hh})}$.

We have used the above effective-mass formulas to optimize our previously published parametrizations of GaAs and GaSb (Ref. 4) for valence- or interband heterostructure calculations. The parameters are listed in Table I, and the gaps and masses they reproduce are given in Table II; included also is a new parametrization for InSb. For reference, Table II also lists the masses and gaps reproduced by our previous parameterization of GaAs. Because the second-nearest-neighbor parameters $V_{xa,ya}$ and $V_{xc,yc}$ affect both the L-valley position and curvature some compromise in the fit of the conduction band is generally necessary. (The less complete experimental picture for InAs and AlSb with respect to both the L valley and [110] and [111] heavy-hole masses, coupled with the fact that their parametrizations in Ref. 4 already reproduce heavy-hole masses similar to those of other III-IV materials suggests leaving these parameter sets unchanged; the AlAs parameter set there reproduces reasonable hole masses given experimental uncertainties.) Here the fitting procedure was much simpler than in the case of Ref. 4, since only the second-nearest-neighbor parameters $V_{xa,ya}$ and $V_{xc,yc}$ were altered. These parameters did not affect the positions or masses of the conduction-band X- and Γ-valleys, and because we are interested here in the valence bands we accepted less accurate L valleys.

The importance of properly fitting the [110] and [111] hole masses is best appreciated by graphing the valence-band

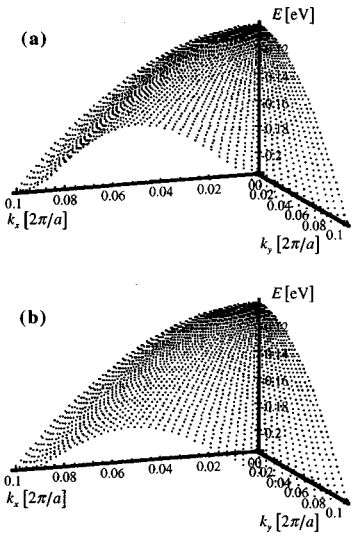

FIG. 1. $E(k_x,k_y,0)$ for one of the heavy-hole bands of GaAs calculated with the parameters of: (a) Ref. 4, and (b) Table I. In both the valence-band maximum is at -0.10278 eV.

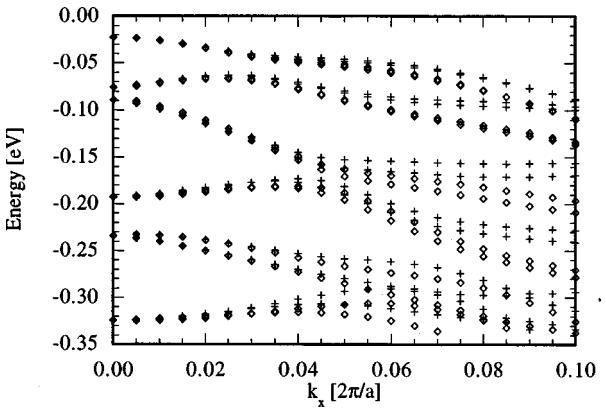

FIG. 2. In-plane dispersion of a symmetric GaAs/AlAs QW with a 20-ML well, calculated with the AlAs parameters of Ref. 4 and the GaAs parameters presented here (diamonds) and in Ref. 4 (crosses). The valence-band maximum for GaAs is at 0.0 eV.

warping. In Fig. 1 we plot $E(k_x,k_y,0)$ for one of the heavy-hole bands of GaAs calculated with: (a) the parameter set of Ref. 4; and (b) the present parameter set. In both cases the valence-band maximum is at $-0.102\,78$ eV; examining Table II we see that although both sets reproduce identical [001] masses their [110] and [111] masses differ significantly. The plots amply illustrate this, since they agree well near the k_x and k_y intercepts, but disagree markedly along the [110] direction. Notice in particular that the larger [110] heavy-hole mass of the earlier parameter set (a) results in too much warping of the heavy-hole bands as compared to the present set (b).

Having seen the effects of the [110] and [111] masses on the bulk bands, we now briefly examine their impact on the in-plane dispersion of a GaAs/AlAs QW, the symmetric structure has 10-ML AlAs barriers and a 20-ML GaAs well. At each value of the in-plane wave vector $\mathbf{k}_\parallel = k_x \mathbf{e}_x$ the subbands are given by the real parts of the poles of the Green function $[E - H(\mathbf{k}_\parallel)]^{-1}$ (Ref. 16), $E_{\rm res}$, under flatband conditions (zero bias and zero-space-charge); the dispersion is obtained by plotting the $(k_x, E_{\rm res})$ pairs. In Fig. 2 we show the subbands of this QW as calculated using the AlAs parameters of Ref. 4 along with the GaAs parameters given here (diamonds) and in Ref. 4 (crosses). The [110] and [111] heavy-hole masses reproduced by the two sets (see Table II) disagree significantly, and this is manifested in the subbands. For very small $k_\parallel$ the subbands agree since these GaAs parameter sets have *identical* [001] masses and the same bandgap, however, for rather modest $k_\parallel$ (essentially above 0.04) they differ significantly. This disagreement underscores the importance of properly fitting the [110] and [111] masses for valence-band quantum heterostructures.

In conclusion, we have examined the spin-orbit sp^3s^* model including interactions up to the second-nearest neighbor, deriving exact analytic expressions for the [110] and [111] heavy- and light-hole masses. We find that, rather surprisingly, the second-nearest-neighbor model affords much more flexibility in fitting the [110] and [111] masses independently of the [001] masses than does the nearest-neighbor model, and that in either model, once both [001] masses and one of the [111] masses are fixed *both* [110] masses, as well as the remaining [111] mass, are *completely determined*; there is no additional freedom in fitting them. We have used these results to alter our earlier conduction-band optimized parameter sets, presenting sets tailored for valence-band structures. Finally, we have seen how the [110] and [111] masses can affect the in-plane dispersion of a QW.

T.B.B. thanks NSF-EPSCoR for support through Alabama EPSCoR Cooperative Agreement No. NSF 9720653. L.J.G. thanks the NSF for support for Students in Optical Sciences and Engineering, Award No. 9553475.

[1] Timothy B. Boykin, Phys. Rev. B **52**, 16 317 (1995).
[2] P. Vogl *et al.*, J. Phys. Chem. Solids **44**, 365 (1983).
[3] Timothy B. Boykin *et al.*, Phys. Rev. B **56**, 4102 (1997).
[4] Timothy B. Boykin, Phys. Rev. B **56**, 9613 (1997). There is a typographical error in Eq. (5): the first term inside the curly braces should read $\rho_a^{l,+}\rho_c^{l,+}V_{x,x}$ (not $V_{x,y}$).
[5] J. P. Loehr and D. N. Talwar, Phys. Rev. B **55**, 4353 (1997).
[6] G. Platero and M. Altarelli, Phys. Rev. B **39**, 3758 (1989).
[7] G. Goldoni and A. Fasolino, Phys. Rev. B **48**, 4948 (1993).
[8] R. K. Hayden *et al.*, Phys. Rev. Lett. **66**, 1749 (1991); R. K. Hayden *et al.*, Appl. Phys. Lett. **61**, 84 (1992).
[9] S. Lin *et al.*, Appl. Phys. Lett. **60**, 601 (1992).
[10] Ulf Gennser *et al.*, Phys. Rev. Lett. **67**, 3828 (1991); Appl. Phys. Lett. **63**, 545 (1993).
[11] A. Zaslavsky *et al.*, Phys. Rev. B **48**, 15 112 (1993).
[12] D. J. Chadi, Phys. Rev. B **16**, 790 (1977).
[13] Timothy B. Boykin, Phys. Rev. B **57**, 1620 (1998).
[14] J. C. Slater and G. F. Koster, Phys. Rev. **94**, 1498 (1954).
[15] In Eq. (1) we rewrite the light-hole/heavy-electron (also heavy-hole/light-electron) coupling term:
$$\frac{V_{x,y}^{\,2}}{E_-^{\rm lh}-E_+^{\rm lh}} = \frac{-V_{x,y}^{\,2}}{2\Delta^{\rm lh}} = -\rho_a^{l,+}\rho_c^{l,+}\frac{V_{x,y}^{\,2}}{V_{x,x}}$$
[16] R. Chris Bowen *et al.*, Phys. Rev. B **52**, 2754 (1995).